iScience

CellPress

Article

CREBH Improves Diet-Induced Obesity, Insulin Resistance, and Metabolic Disturbances by FGF21-Dependent and FGF21-Independent Mechanisms

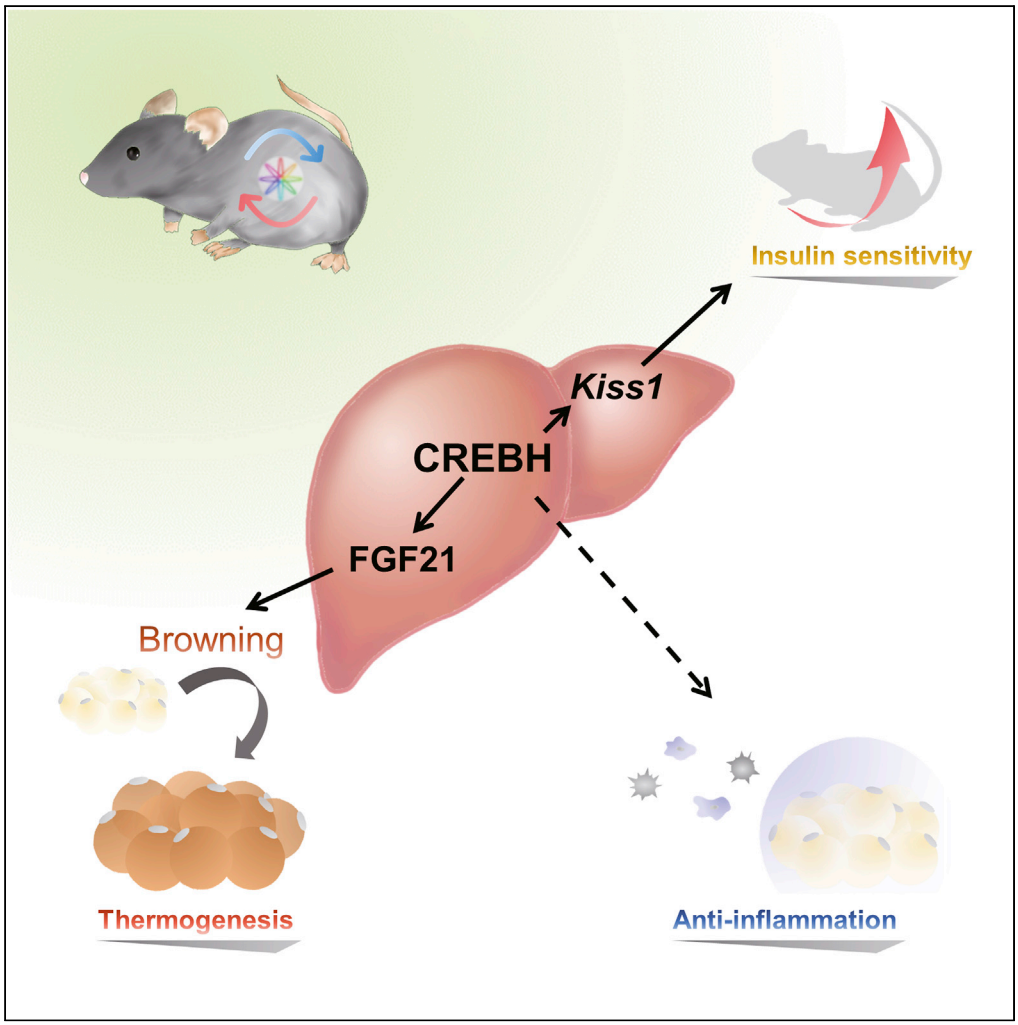

Aoi Satoh, Songiee Han, Masaya Araki, ..., Takashi Matsuzaka, Hirohito Sone, Hitoshi Shimano

ynakagawa@md.tsukuba.ac.jp (Y.N.)
hshimano@md.tsukuba.ac.jp (H.S.)

HIGHLIGHTS

Deficiency of FGF21 in CREBH-Tg mice mostly cancels the improvement of obesity

CREBH induces browning in iWAT

CREBH suppresses inflammation of eWAT

CREBH-induced Kiss1 contributes to improvement of glucose metabolism

DATA AND CODE AVAILABILITY

GSE143420
GSE143421

Satoh et al., iScience *23*, 100930
March 27, 2020
https://doi.org/10.1016/j.isci.2020.100930

iScience

CellPress

Article

CREBH Improves Diet-Induced Obesity, Insulin Resistance, and Metabolic Disturbances by FGF21-Dependent and FGF21-Independent Mechanisms

Aoi Satoh,[1,8] Song-iee Han,[1,2,8] Masaya Araki,[1,8] Yoshimi Nakagawa,[1,2,*] Hiroshi Ohno,[1] Yuhei Mizunoe,[1] Kae Kumagai,[1] Yuki Murayama,[1] Yoshinori Osaki,[1] Hitoshi Iwasaki,[1] Motohiro Sekiya,[1] Morichika Konishi,[3] Nobuyuki Itoh,[4] Takashi Matsuzaka,[1] Hirohito Sone,[5] and Hitoshi Shimano[1,2,6,7,9,*]

SUMMARY

Mice overexpressing the nuclear form of CREBH mainly in the liver (CREBH-Tg) showed suppression of high-fat high-sucrose (HFHS) diet-induced obesity accompanied by an increase in plasma fibroblast growth factor 21 (FGF21) levels. CREBH overexpression induced browning in inguinal white adipose tissue (WAT) and whole-body energy expenditure, which was canceled in *Fgf21*$^{-/-}$ mice. Deficiency of FGF21 in CREBH-Tg mice mostly canceled the improvement of obesity, but the suppression of inflammation of epidermal WAT, amelioration of insulin resistance, and improvement of glucose metabolism still sustained. Kisspeptin 1 (*Kiss1*) was identified as a novel hormone target for CREBH to explain these FGF21-independent effects of CREBH. Knockdown of Kiss1 in HFHS-fed CREBH-Tg *Fgf21*$^{-/-}$ mice showed partially canceled improvement of glucose metabolism. Taken together, we propose that hepatic CREBH pleiotropically improves diet-induced obesity-mediated dysfunctions in peripheral tissues by improving systemic energy metabolism in FGF21-dependent and FGF21-independent mechanisms.

INTRODUCTION

cAMP responsive element-binding protein 3-like 3 (CREB3L3, also named CREBH) is a basic liver-specific leucine zipper transcription factor belonging to the CREB/ATF family (Omori et al., 2001). CREBH predominantly resides in the endoplasmic reticulum (ER). Under ER stress, CREBH is transferred to the Golgi apparatus where site 1 and site 2 proteases cleave its amino-terminal portion with its subsequent transfer to the nucleus to induce its target genes (Zhang et al., 2006). *CrebH* expression in the liver is induced in a fasted state rather than the fed state, resulting in accumulation of the nuclear form of CREBH. Previously, our group reported that transgenic mice overexpressing the nuclear form of CREBH in the liver (CREBH-Tg) resist diet-induced obesity (DIO) by remarkably increasing hepatic gene expression and plasma levels of fibroblast growth factor 21 (FGF21) (Nakagawa et al., 2014). CREBH-Tg mice also present improvements in hyperlipidemia, hyperglycemia, and insulin resistance in DIO mice (Nakagawa et al., 2014). Conversely, CREBH knockout (KO) (*CrebH*$^{-/-}$) mice exhibit hypertriglyceridemia due to inefficient catalysis of triglyceride (TG) clearance by lipoprotein lipase (LPL) in blood. Hypertriglyceridemia results from the reduction of the expression of the LPL coactivators, Apolipoprotein c2 (*Apoc2*), *Apoa4*, and *Apoa5*, and the increase of the LPL inhibitor *Apoc3* in the liver (Lee et al., 2011; Zhang et al., 2012). When fed a methionine-choline-deficient diet or ketogenic diet (KD), the deficiency of CREBH results in hepatic steatosis (Nakagawa et al., 2016a, 2016b; Park et al., 2016).

FGF21 is a unique member of the FGF family. It has hormone-like actions and is a key mediator of starvation by activating fatty acid oxidation and ketogenesis in the liver and lipolysis in white adipose tissue (WAT) (Badman et al., 2007; Inagaki et al., 2007). FGF21 is mainly synthesized in the liver, and adipose tissues are also important organs for both the production and activity of FGF21. In adipocytes, FGF21 enhances insulin-independent glucose uptake, promotes mitochondrial oxidation, and induces secretion of adiponectin, which in turn mediates the glucose-lowering and insulin-sensitizing effects of FGF21 (Chau et al., 2010; Lin et al., 2013). In response to the cold challenge, FGF21 is induced in adipose tissues, but not in the liver (Fisher et al., 2012; Hondares et al., 2011). Deficiency of FGF21 in mice impairs cold-induced browning of inguinal WAT (iWAT), whereas recombinant FGF21 administration increases browning of iWAT and total energy expenditure in mice (Fisher et al., 2012). Recently, it was reported that plasma

[1]Department of Internal Medicine (Endocrinology and Metabolism), Faculty of Medicine, University of Tsukuba, 1-1-1 Tennodai, Tsukuba, Ibaraki 305-8575, Japan

[2]International Institute for Integrative Sleep Medicine (WPI-IIIS), University of Tsukuba, 1-1-1 Tennodai, Tsukuba, Ibaraki 305-8575, Japan

[3]Laboratory of Microbial Chemistry, Kobe Pharmaceutical University, 4-19-1, Motoyamakitamachi, Higashinada-Ku, Kobe, Hyogo, 658-8558, Japan

[4]Department of Genetic Biochemistry, Graduate School of Pharmaceutical Science, Kyoto University, 46-29 Yoshida-Shimoadachi-Cho, Sakyo-ku, Kyoto, Kyoto 606-8501, Japan

[5]Department of Hematology, Endocrinology and Metabolism, Niigata University Faculty of Medicine, 757 Asahimachi, Niigata, Niigata 951-8510, Japan

[6]Life Science Center for Survival Dynamics, Tsukuba Advanced Research Alliance (TARA), University of Tsukuba, 1-1-1 Tennodai, Tsukuba, Ibaraki 305-8577, Japan

[7]Japan Agency for Medical Research and Development–Core Research for Evolutional Science and Technology (AMED-CREST), 1-7-1 Otemachi, Chiyoda-ku, Tokyo, Japan

[8]These authors contributed equally

[9]Lead Contact

Continued

FGF21 levels positively correlate with the weight of iWAT in insulin-sensitive obese individuals (Li et al., 2018). *Fgf21*$^{-/-}$ mice show less iWAT mass and are more insulin resistant when fed a high-fat diet. Plasma FGF21 upregulates adiponectin in iWAT, accompanied by an increase of M2 macrophage polarization (Li et al., 2018). The upregulation of plasma FGF21 levels in obesity is thought to serve as a defense mechanism to protect against systemic insulin resistance (Li et al., 2018). FGF21 is proposed to have therapeutic effects on obesity-related metabolic disturbances, such as insulin resistance, diabetes, and hypertriglyceridemia in *ob/ob* mice, DIO mice, and diabetic monkeys (Kharitonenkov et al., 2007; Xu et al., 2009). Similar to insulin resistance, FGF21 resistance is induced in obese mice such as DIO and *ob/ob* mice, thereby increasing plasma FGF21 levels (Fisher et al., 2010). This contributed to a decrease of βKlotho in WAT, but not in the liver of obese mice (Fisher et al., 2010). *Fgf21* expression is governed by peroxisome proliferator-activated receptor (PPAR) α and CREBH, which is induced by fasting or KD feeding (Badman et al., 2007; Inagaki et al., 2007; Nakagawa et al., 2014, 2016b). Both CREBH and PPARα are activated in an autoloop manner in response to starvation, and thus synergistically activate *Fgf21* expression (Kim et al., 2014; Nakagawa et al., 2014).

Previously, we proposed that CREBH-Tg mice ameliorate the pathology of DIO mice by inducing hepatic expression and plasma levels of FGF21. In this study, by using *Fgf21*$^{-/-}$ mice, we identified the FGF21-dependent or FGF21-independent effects on CREBH-mediated improvement of obesity.

RESULTS

FGF21 Has a Crucial Role in the Suppression of Diet-Induced Obesity in CREBH-Tg Mice

In CREBH-Tg mice, body weight (BW) gain, hyperglycemia, hyperinsulinemia, and hypertriglyceridemia are clearly suppressed relative to high-fat high-sucrose (HFHS) DIO (Nakagawa et al., 2014). There is a possibility that these phenotypes of CREBH-Tg mice are a result of hepatic induction of *Fgf21*, a CREBH target gene (Nakagawa et al., 2014). To determine this notion, we generated CREBH-Tg *Fgf21*$^{-/-}$ mice by crossing CREBH-Tg mice with *Fgf21*$^{-/-}$ mice and then fed them with HFHS diet for 12 weeks. Consistent with the previous report (Nakagawa et al., 2014), BW gain was suppressed in CREBH-Tg mice compared with control wild-type (WT) mice following HFHS diet (Figure 1A). In contrast, BW of CREBH-Tg *Fgf21*$^{-/-}$ mice was reversed to the levels of WT mice, although *Fgf21*$^{-/-}$ mice did not show a significant increase in BW compared with WT mice (Figure 1A). There were no differences in liver weight among WT, CREBH-Tg, and CREBH-Tg *Fgf21*$^{-/-}$ mice, whereas *Fgf21*$^{-/-}$ mice had a higher liver weight than WT mice (Figure 1B). In accordance with BW changes, CREBH-Tg mice exhibited significantly lower epidermal WAT (eWAT) weight than WT mice but CREBH-Tg *Fgf21*$^{-/-}$mice did not (Figure 1B). Thus, suppressive effect of CREBH overexpression on DIO was completely canceled out in CREBH-Tg *Fgf21*$^{-/-}$ mice, indicating that fat loss effect of CREBH on a quantitative basis was mostly mediated through FGF21. There were no differences in food intake among all the groups (Figure 1C).

CREBH Overexpression Showed FGF21-Dependent Suppression of HFHS Diet-Induced Lipid Accumulation in the Liver and FGF21-Independent Amelioration of Insulin Resistance

CREBH overexpression in WT mice was associated with a significant reduction in plasma glucose, insulin, and TG levels, whereas there were no differences in plasma total cholesterol (TC) and nonesterified fatty acid (NEFA) levels compared with WT mice (Figures 1D and 1E). Meanwhile, *Fgf21*$^{-/-}$ mice showed no changes in plasma glucose or NEFA levels compared with WT mice, but had a tendency to increase plasma insulin levels, indicating insulin resistance (Figures 1D and 1E). Then, plasma glucose levels of CREBH-Tg *Fgf21*$^{-/-}$ mice did not significantly change compared with those of CREBH-Tg mice or *Fgf21*$^{-/-}$ mice, but CREBH-Tg *Fgf21*$^{-/-}$ mice sustained significantly reduced plasma insulin levels (similar to CREBH-Tg mice and significantly lower than that of *Fgf21*$^{-/-}$ mice) (Figure 1D). The data indicated that unlike obesity, amelioration of insulin resistance by CREBH overexpression is at least partially FGF21 independent. CREBH-Tg *Fgf21*$^{-/-}$ mice showed no marked further changes in TG, TC, and NEFA levels compared with their respective controls (Figure 1E). Consistent with a previous report (Nakagawa et al., 2014), plasma FGF21 levels in CREBH-Tg mice were apparently increased compared with WT mice (Figure 1F). Morphological analysis with hematoxylin and eosin staining in the liver revealed that CREBH-Tg mice clearly had fewer and smaller lipid droplets compared with WT mice (Figure 1G). *Fgf21*$^{-/-}$ mice exhibited exacerbation of hepatosteatosis with larger lipid droplets than WT mice. Additional absence of FGF21 in CREBH-Tg canceled amelioration of hepatosteatosis, but CREBH-Tg *Fgf21*$^{-/-}$ mice had still smaller lipid droplets than *Fgf21*$^{-/-}$ mice (Figure 1G). Consistently, the quantitative analysis revealed that liver TG was significantly reduced in CREBH-Tg mice and significantly increased in *Fgf21*$^{-/-}$ mice compared with WT mice

*Correspondence:
ynakagawa@md.tsukuba.ac.jp (Y.N.),
hshimano@md.tsukuba.ac.jp (H.S.)

https://doi.org/10.1016/j.isci.2020.100930

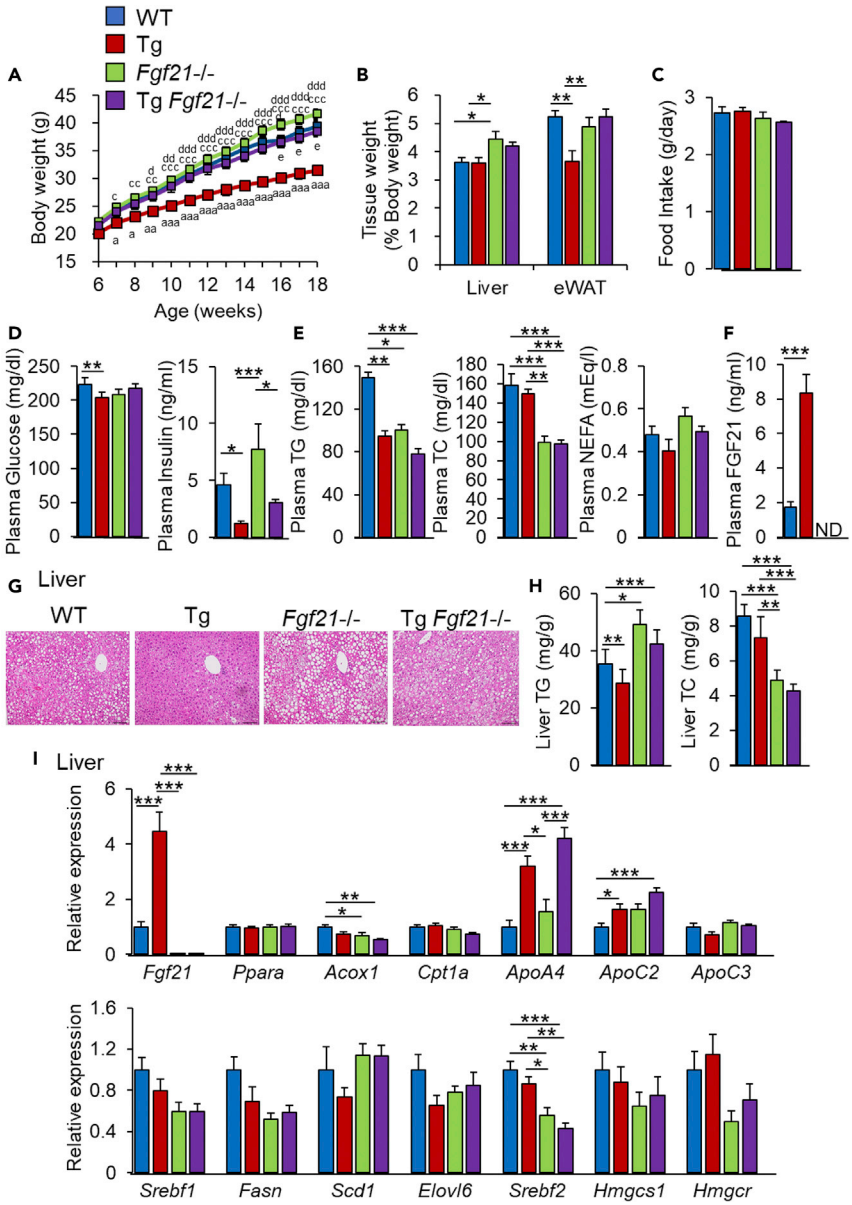

Figure 1. CREBH-Tg Mice Show Improvement of Diet-Induced Obesity

Six-week-old male WT, Tg, *Fgf21*$^{-/-}$, and Tg *Fgf21*$^{-/-}$ mice were fed a high-fat high-sucrose (HFHS) diet for 12 weeks.

(A) Body weight changes at indicated ages (n = 14–26 per group). [a]Statistical significance between WT and Tg mice ([a]$p < 0.05$, [aa]$p < 0.01$, [aaa]$p < 0.001$). [b]Statistical significance between WT and *Fgf21*$^{-/-}$ mice ([b]$p < 0.05$). [c]Statistical significance between Tg and *Fgf21*$^{-/-}$ mice ([c]$p < 0.05$, [cc]$p < 0.01$, [ccc]$p < 0.001$). [d]Statistical significance between Tg and Tg *Fgf21*$^{-/-}$ mice ([d]$p < 0.05$, [dd]$p < 0.01$, [ddd]$p < 0.001$). [e]Statistical significance between *Fgf21*$^{-/-}$ and Tg *Fgf21*$^{-/-}$ mice ([e]$p < 0.05$).

(B) Liver and epidermal WAT (eWAT) weights (n = 8–13).

(C) Food intake (n = 4–7).

(D) Plasma levels of glucose and insulin (n = 8–22).

(E) Plasma levels of triglyceride (TG), total cholesterol (TC), and nonesterified fatty acids (NEFA) (n = 9–14).

(F) Plasma levels of FGF21 (n = 11–12).

(G) Representative pictures of liver sections stained with H&E.

(H) Liver TG and TC (n = 9–14).

(I) mRNA expressions of CREBH target genes, lipid, and cholesterol synthetic genes in livers were determined by real-time PCR (n = 7–12). Results are represented as means ± SEM. *$p < 0.05$, **$p < 0.01$, ***$p < 0.001$.

(Figure 1H). Liver TG content of CREBH-Tg *Fgf21*$^{-/-}$ mice had a trend to decrease compared with *Fgf21*$^{-/-}$ mice (Figure 1H). Liver TC content significantly decreased in *Fgf21*$^{-/-}$ mice compared with WT mice, but no further reduction in CREBH-Tg *Fgf21*$^{-/-}$ mice was observed (Figure 1H).

CREBH Increased *Fgf21* and *Apoa4* Expression in the Liver of DIO Mice

Consistent with the elevated plasma FGF21 levels (Figure 1F), CREBH overexpression significantly increased hepatic *Fgf21* expression compared with control WT mice and was undetectable in *Fgf21*$^{-/-}$ background mice (Figure 1I). CREBH overexpression increased target gene expression of *Apoa4* and *Apoc2*, activators for LPL (Figure 1I), which contributes to a reduction in plasma TG levels. CREBH-Tg mice had a trend to reduce *Srebp-1c* expression and subsequently reduce its target gene expression of fatty acid synthase (*Fasn*) and stearoyl-coenzyme A desaturase 1 (*Scd1*) and elongation of very-long-chain fatty acid (FEN1/Elo2, SUR4/Elo3, yeast)-like 6 (*Elovl6*) in the liver compared with WT mice (Figure 1I). For cholesterol synthesis genes including *Srebf2*, 3-hydroxy-3-methylglutaryl-CoA synthase 1 (*Hmgcs1*) and 3-hydroxy-3-methylglutaryl-CoA reductase (*Hmgcr*), CREBH overexpression had no effects in both control WT and *Fgf21*$^{-/-}$ mice (Figure 1I). FGF21 reciprocally changed liver TG and TC contents, whereas the effects of CREBH on hepatic lipogenic and cholesterogenic gene expression were marginal.

CREBH Induces Browning in iWAT of DIO Mice

Browning is the appearance and activation of beige adipocytes within iWAT, accompanied by induction of UCP1 (Veniant et al., 2015). As CREBH-Tg mice showed suppression of DIO-induced adiposity, we determined the changes in gene expression related to browning and lipolysis in WATs, including eWAT, iWAT, and brown adipose tissue (BAT) of each DIO mice group. Although the previous report indicated that FGF21 activates lipolysis in WATs (Hotta et al., 2009), lipolysis-related genes such as lipase and hormone-sensitive (*lipe*) and patatin-like phospholipase domain-containing 2 (*Pnpla2*) in WATs and BATs were not apparently changed by CREBH overexpression despite high plasma FGF21 levels (Figures 2A–2C). Meanwhile, gene profile in eWAT among four groups highlighted browning markers, uncoupling protein 1 (*Ucp1*), *Elovl3*, and cell death-inducing DNA fragmentation factor alpha-like effector A (*Cidea*). *Ucp1* and *Elovl3* expression was significantly increased in *Fgf21*$^{-/-}$ mice, which were suppressed in CREBH-Tg *Fgf21*$^{-/-}$ mice (Figure 2A). In contrast, CREBH overexpression in both control WT and *Fgf21*$^{-/-}$ mice significantly increased *Cidea* expression in eWAT, which implicates FGF21-independent CREBH-specific effect on browning (Figure 2A). In iWAT, CREBH-Tg mice showed a significant increase in several browning-induced genes such as peroxisome proliferative-activated receptor, gamma, coactivator 1 alpha (*Ppargc1a*), and *Cidea*, and the subsequent increase in *Ucp1* compared with WT mice (Figure 2B), indicating that CREBH-Tg mice might induce browning and thermogenesis in iWAT. These changes were partially canceled in CREBH-Tg *Fgf21*$^{-/-}$ mice, but the increase in *Ucp1* and *Cidea* were still partially maintained (Figure 2B), suggesting that CREBH-induced browning of iWAT is both FGF21 dependent and FGF21 independent presumably depending on details in browning functions. *Elovl3*, a mitochondrial function marker, was markedly increased in CREBH-Tg mice, which was completely canceled in CREBH-Tg *Fgf21*$^{-/-}$ mice (Figure 2B). These results indicate that CREBH induces browning genes in iWAT by FGF21-dependent and FGF21-independent mechanisms. However, PR domain containing 16 (*Prdm16*), a master regulator for brown adipocyte differentiation, was not apparently changed in CREBH-Tg mice, indicating that CREBH-induced browning is independent of mediating the expression of PRDM16. Regarding lipolysis, *Pnpla2*, not *lipe*, was slightly increased in iWAT of CREBH-Tg mice, which was canceled in CREBH-Tg *Fgf21*$^{-/-}$ mice (Figure 2B). In BAT, *Ucp1* and browning genes remained unchanged in WT and CREBH-Tg mice (Figure 2C). However, *Elovl3* expression was significantly induced in BAT of CREBH-Tg mice (Figure 2C), activating mitochondrial function and energy expenditure. This change was blunted in *Fgf21*$^{-/-}$ background mice groups (Figure 2C), indicating that FGF21 governs *Elovl3* expression in BAT.

We investigated UCP1 regulation at the protein level. Consistent with gene expression, UCP1 protein levels were markedly upregulated in the iWAT of CREBH-Tg mice compared with WT mice, whereas robust UCP1 protein contents in BAT were not changed between WT and CREBH-Tg mice (Figure 2D). In eWAT, UCP1 proteins were not detected (Figure 2D). FGF21 is known to induce UCP1 protein in iWAT (Fisher et al., 2012); thus, we evaluated it in CREBH-Tg *Fgf21*$^{-/-}$ mice. The induction of UCP1 in iWAT of CREBH-Tg mice was canceled in CREBH-Tg *Fgf21*$^{-/-}$ mice (Figure 2E). The induction of UCP1 in iWAT of CREBH-Tg mice was confirmed by immunocytochemistry using UCP1 antibodies (Figure 2F). These findings support the presumption that the induction of UCP1 in CREBH-Tg mice is mediated by FGF21.

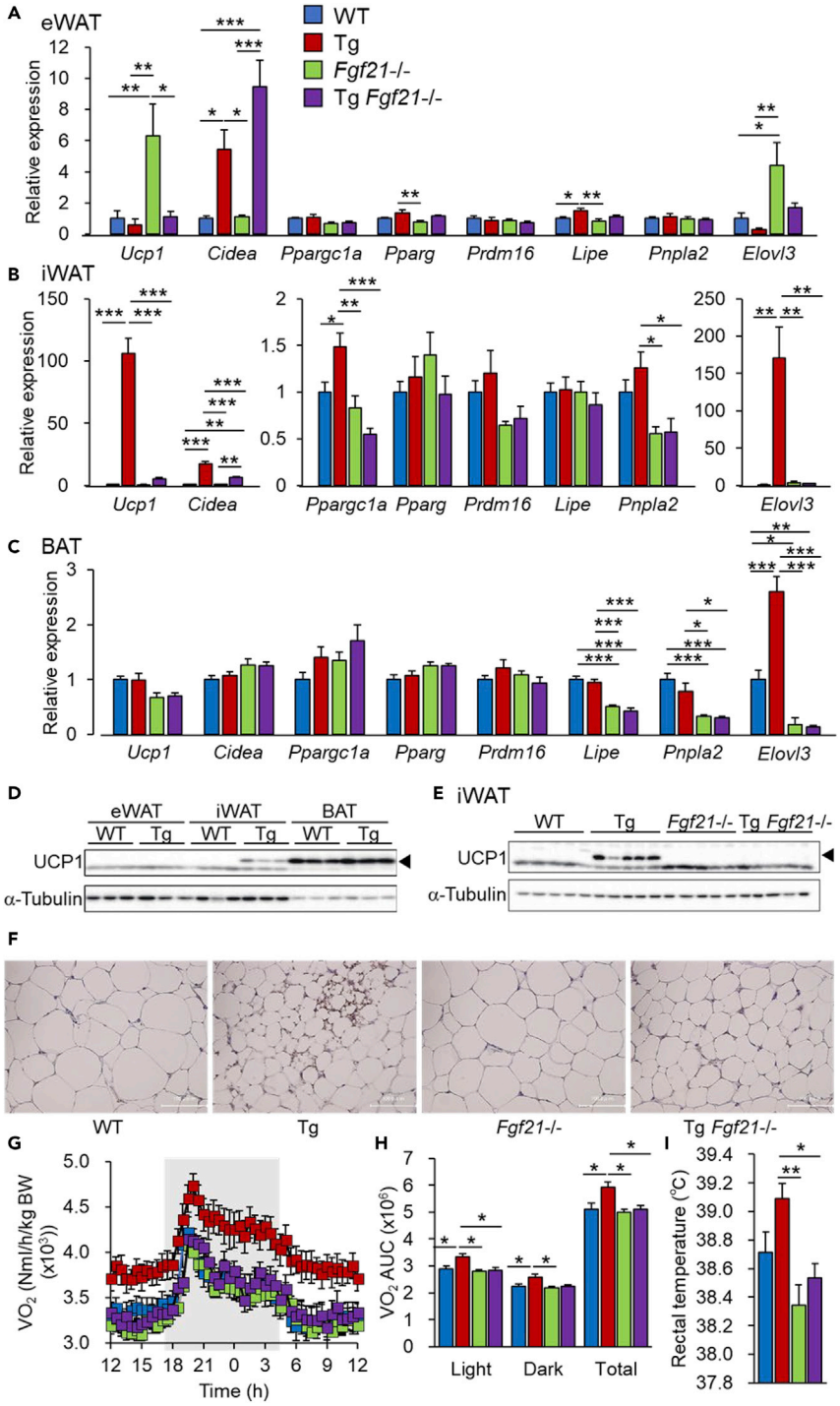

Figure 2. CREBH-Tg Mice Induce Browning in Inguinal WAT (iWAT) via FGF21

Six-week-old male WT, Tg, *Fgf21*$^{-/-}$, and Tg *Fgf21*$^{-/-}$ mice were fed an HFHS diet for 2 weeks.

(A–C) mRNA expressions of beige adipocyte marker genes in epidermal WAT (eWAT) (A), iWAT (B), and brown adipose tissue (BAT) (C) were determined by real-time PCR (n = 4–8).

(D) UCP1 protein expression in eWAT, iWAT, and BAT from WT and Tg mice; α-tubulin was used as a loading control (n = 3).

(E) UCP1 protein expression in iWAT from WT, Tg, *Fgf21*$^{-/-}$, and Tg *Fgf21*$^{-/-}$ mice; α-tubulin was used as a loading control (n = 5).

(F) UCP1 immunostaining of iWAT from WT and Tg mice.

Figure 2. *Continued*

(G) Oxygen consumption VO_2 (NmL/h/kg) of WT, Tg, *Fgf21*$^{-/-}$, and Tg *Fgf21*$^{-/-}$ mice measured by the ARCO2000 System (Arcosystem) (n = 5–9).

(H) The areas under the curve (AUCs) from the light, dark, and total periods in (F) (n = 5–9).

(I) Rectal core temperature of WT, Tg, *Fgf21*$^{-/-}$, and Tg *Fgf21*$^{-/-}$ mice (n = 8–14). Results are represented as means ± SEM. *p < 0.05, **p < 0.01, ***p < 0.001.

CREBH Induces Whole-Body O_2 Consumption Depending on FGF21

As it is predicted that thermogenesis is activated in CREBH-Tg mice, we determined the energy expenditure. The energy expenditure of 6-week-old mice fed an HFHS diet for 2 weeks was determined. Consistent with the induction of browning in iWAT, CREBH-Tg mice had higher O_2 consumption than control WT mice throughout the day (Figures 2G and 2H). CREBH-Tg mice tended to have a higher body temperature than control WT mice (Figure 2I). These changes by CREBH overexpression were canceled in *Fgf21*$^{-/-}$ background mice (Figures 2G–2I). These results indicate that CREBH resists DIO by enhancing basal metabolism and especially thermogenesis, which is dependent on FGF21.

CREBH Overexpression Improves Both Glucose Response and Insulin Response in WT and Even *Fgf21*$^{-/-}$ Mice

Improvement of diet-induced insulin resistance by CREBH overexpression (Figure 1D) was further investigated by performing glucose tolerance test (GTT) and insulin tolerance test (ITT) in WT, CREBH-Tg, *Fgf21*$^{-/-}$, and CREBH-Tg *Fgf21*$^{-/-}$ mice fed an HFHS diet. In GTT, plasma glucose levels of *Fgf21*$^{-/-}$ mice were higher than those of other groups, but other groups showed no differences in plasma glucose levels during GTT (Figure 3A). These changes were confirmed by calculating the area under the curve (Figure 3A). The data indicate that CREBH overexpression did not change glucose tolerance following an HFHS diet but ameliorated impairment by FGF21 absence. Intriguingly, plasma insulin levels of CREBH-Tg *Fgf21*$^{-/-}$ mice were lower than those of WT mice but were higher than those of CREBH-Tg mice, indicating marked improvement in insulin resistance by overexpression of CREBH even in the absence of *Fgf21* (Figure 3B). Homeostasis model assessment of insulin resistance also showed that CREBH overexpression improves insulin resistance in WT and even *Fgf21*$^{-/-}$ mice (Figure 3C). ITT demonstrated that the slightly slurred insulin response curve of WT mice on HFHS diet was markedly reduced in CREBH-Tg mice so that almost no increment in insulin response was necessary to maintain similar glucose excursion of WT mice (Figure 3D), indicating a profound improvement of insulin sensitivity. Similarly, CREBH-Tg *Fgf21*$^{-/-}$ mice had lower plasma glucose levels than that of control WT and even *Fgf21*$^{-/-}$ mice (Figure 3D). In contrast to dependence on FGF21 in amelioration of DIO, CREBH overexpression can also promote insulin response by both FGF21-dependent and FGF21-independent mechanisms with the latter more marked.

CREBH-Tg Mice Showed Suppression of HFHS Diet-Induced Macrophage Infiltration in eWAT

Histological analysis of eWAT using hematoxylin and eosin staining indicated that *Fgf21*$^{-/-}$ mice had cell size of eWAT similar to WT mice; CREBH overexpression WT and *Fgf21*$^{-/-}$ mice reduced this (Figure 4A). Interestingly, immunohistochemistry using antibody against F4/80 in eWAT showed that *Fgf21*$^{-/-}$ mice induced infiltrated macrophages compared with WT mice and CREBH overexpression reduced them compared with WT and even *Fgf21*$^{-/-}$ mice (Figure 4A). As FGF21 is reported to suppress inflammation in eWAT (Wang et al., 2018), deficiency of FGF21 increased expression of genes such as CD68 antigen (*Cd68*), tumor necrosis factor (*Tnf*), chemokine (C-C motif) ligand 2 (*Ccl2*), and interleukin-6 (*Il6*) compared with WT mice (Figure 4B). These changes were consistent with an increase of macrophage infiltration in eWAT of *Fgf21*$^{-/-}$ mice shown in Figure 4A. CREBH overexpression in both WT and *Fgf21*$^{-/-}$ mice reduced the macrophage marker *Cd68* and inflammatory genes such as *Ccl2* and *Tnf* compared with WT and *Fgf21*$^{-/-}$ mice, respectively (Figure 4B). Furthermore, CREBH overexpression significantly decreased *Il6* expression in *Fgf21*$^{-/-}$ mice, and there were no changes in WT mice (Figure 4B). Therefore, the data support the fact that anti-inflammatory effects of CREBH might be FGF21 independent. BAT adipocytes of WT and *Fgf21*$^{-/-}$ mice exhibited larger and unilocular lipid droplets like a WAT adipocyte (Figure 4C). CREBH overexpression suppressed these changes in both WT and *Fgf21*$^{-/-}$ mice (Figure 4C). These findings suggest that the suppressive effects of CREBH on lipid accumulation in BAT are FGF21 independent. It has been known that inflammation in eWAT and BAT is associated with insulin resistance, and these observations could be a part of the FGF21-independent insulin sensitization by CREBH.

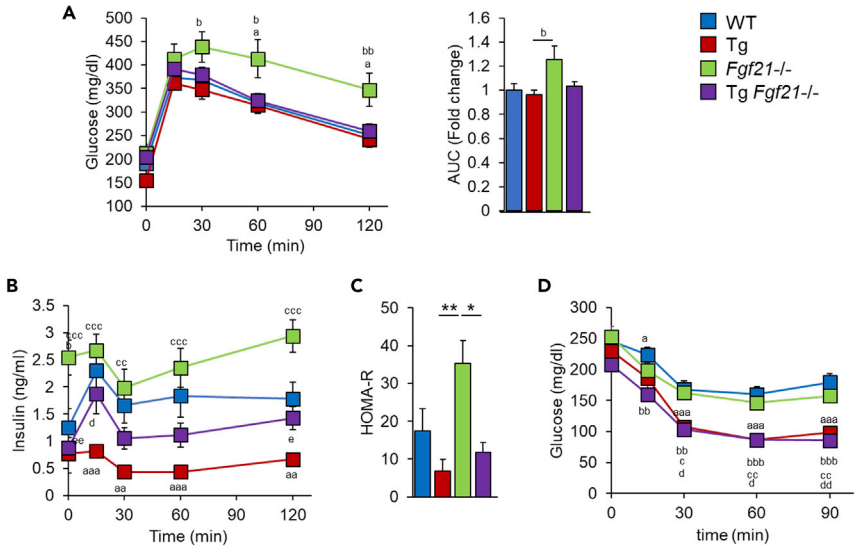

Figure 3. CREBH-Tg Mice Prevent HFHS-Induced Insulin Resistance Independent of FGF21

(A) Plasma glucose levels during glucose tolerance test (GTT) in WT, Tg, *Fgf21*$^{-/-}$, and Tg *Fgf21*$^{-/-}$ mice fed 12 weeks of HFHS diet from age 6 weeks (left) and AUC (right) (n = 7–24). [a]Statistical significance between WT and *Fgf21*$^{-/-}$ mice ([a]$p < 0.05$). [b]Statistical significance between Tg and *Fgf21*$^{-/-}$ mice ([b]$p < 0.05$, [bb]$p < 0.01$).

(B) Plasma insulin levels during GTT (n = 7–18). [a]Statistical significance between WT and Tg mice ([aa]$p < 0.01$, [aaa]$p < 0.001$). [b]Statistical significance between WT and *Fgf21*$^{-/-}$ mice ([b]$p < 0.05$). [c]Statistical significance between Tg and *Fgf21*$^{-/-}$ mice ([cc]$p < 0.01$, [ccc]$p < 0.001$). [d]Statistical significance between Tg and Tg *Fgf21*$^{-/-}$ mice ([d]$p < 0.05$). [e]Statistical significance between *Fgf21*$^{-/-}$ and Tg *Fgf21*$^{-/-}$ mice ([e]$p < 0.05$, [ee]$p < 0.01$).

(C) The homeostatic model assessment index of insulin resistance (HOMA-R) in WT, Tg, *Fgf21*$^{-/-}$, and Tg *Fgf21*$^{-/-}$ mice fed HFHS diet for 12 weeks from age 6 weeks (n = 7–18). *$p < 0.05$, **$p < 0.01$.

(D) Blood glucose levels during insulin tolerance test (ITT) in WT, Tg, *Fgf21*$^{-/-}$, and Tg *Fgf21*$^{-/-}$ mice fed normal chow diet for 12 weeks from age 6 weeks (n = 9–25). [a]Statistical significance between WT and Tg mice ([a]$p < 0.05$, [aaa]$p < 0.001$). [b]Statistical significance between WT and Tg *Fgf21*$^{-/-}$ mice ([bb]$p < 0.01$, [bbb]$p < 0.001$). [c]Statistical significance between Tg and *Fgf21*$^{-/-}$ mice ([c]$p < 0.05$, [cc]$p < 0.01$). [d]Statistical significance between *Fgf21*$^{-/-}$ and Tg *Fgf21*$^{-/-}$ mice ([d]$p < 0.05$, [dd]$p < 0.01$). Results are represented as means ± SEM.

CREBH Ameliorates Glucose Metabolism in *ob/ob* Mice, a Type 2 Diabetic Mouse Model, and FGF21-Resistant Mice

Another obese, but genetic, mouse model, *ob/ob* mice, showed FGF21 resistance with an expected and marked increase in plasma FGF21 levels (Fisher et al., 2010; Hale et al., 2012). If *ob/ob* mice overexpressing CREBH improve the pathology, it would suggest that CREBH has other target genes to ameliorate metabolic disorder except for FGF21. CREBH-Tg mice were crossed with *ob/ob* mice. There were no apparent differences in BW changes between *ob/ob* and *ob/ob*; CREBH-Tg mice (data not shown). As expected, *ob/ob* mice had higher hepatic *Fgf21* expression and plasma FGF21 levels compared with ob/+ control mice (Figures 5A and 5B). *ob/ob*; CREBH-Tg mice had a trend to increase hepatic gene expression and plasma levels of FGF21 compared with *ob/ob* mice (Figures 5A and 5B). *ob/ob*; CREBH-Tg mice showed a significant reduction in plasma glucose and insulin levels compared with *ob/ob* mice (Figures 5C and 5D). Although *ob/ob* mice have FGF21 resistance, CREBH-induced FGF21 might contribute to an improvement in glucose metabolism in *ob/ob*; CREBH-Tg mice. In GTT, CREBH overexpression in *ob/ob* mice markedly reduced plasma glucose and insulin levels compared with *ob/ob* mice (Figures 5E and 5F), indicating that glucose intolerance was improved in *ob/ob*; CREBH-Tg mice. In ITT, plasma glucose levels of *ob/ob*; CREBH-Tg mice were lower than in *ob/ob* mice, indicating that CREBH overexpression can improve insulin resistance (Figure 5G). Collectively, an improvement in glucose metabolism in CREBH overexpression in *ob/ob* mice despite FGF21 resistance was another piece of evidence that CREBH ameliorates insulin resistance regardless of FGF21.

Kiss1 as a Novel CREBH Target Gene in the Liver

To identify novel CREBH target genes, except for FGF21, which improves insulin sensitivity, we analyzed a combination of two different microarray datasets. One was the ratio of HFHS diet-fed CREBH-Tg to WT mice liver

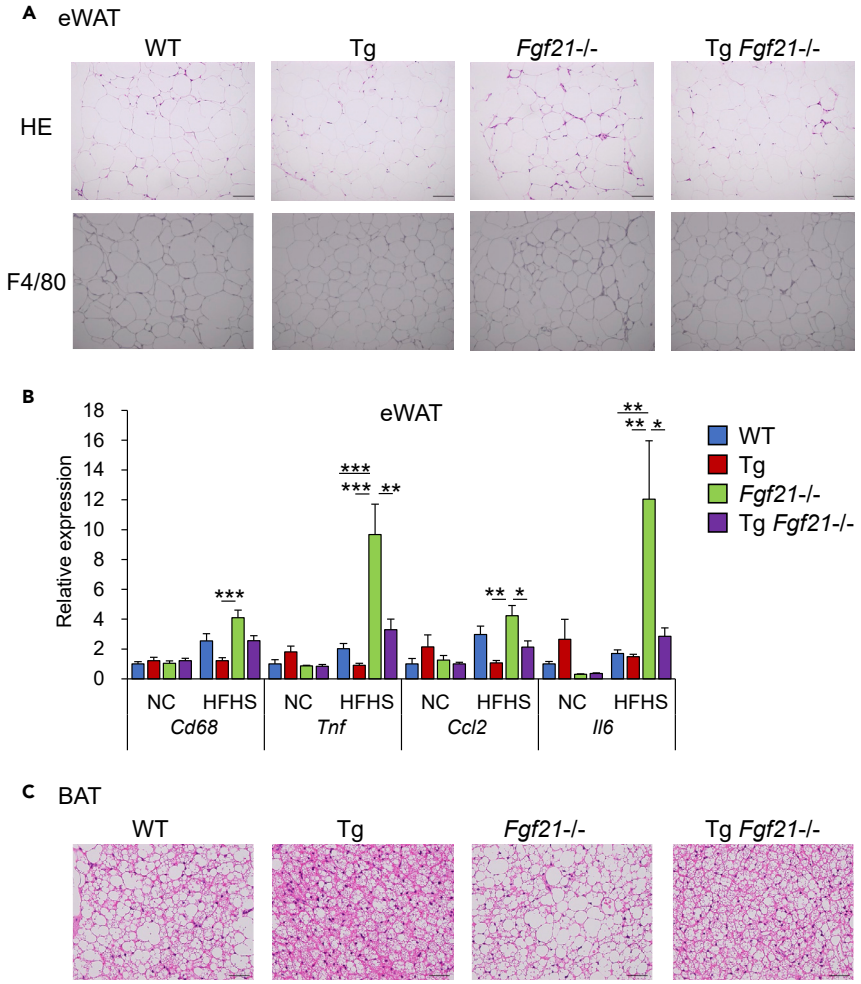

Figure 4. CREBH-Tg Mice Suppress the Inflammation in eWAT and Lipid Accumulation in BAT Independent of FGF21

(A and C) Representative pictures of (A) epidermal WAT (eWAT) sections stained with H&E (upper) and F4/80 immunostaining (bottom) and (C) brown adipose tissue (BAT) sections stained with H&E from WT, Tg, *Fgf21*$^{-/-}$, and Tg *Fgf21*$^{-/-}$ mice fed an HFHS diet for 12 weeks from age 6 weeks.

(B) Six-week-old male WT, Tg, *Fgf21*$^{-/-}$, and Tg *Fgf21*$^{-/-}$ mice were fed a normal chow or HFHS diet for 12 weeks. mRNA expressions of inflammatory genes in eWAT were determined by real-time PCR (n = 7–8). Results are represented as means ± SEM. *p < 0.05, **p < 0.01, ***p < 0.001.

samples (x axis), and the other was the ratio of fed state to the fasted state (y axis) based upon the observation that CREBH is activated physiologically at fasting (Figure 6A) (Danno et al., 2010). We identified Kisspeptin (Kiss1), a neuropeptide secreted by the liver and brain (Gottsch et al., 2004; Song et al., 2014), as a candidate CREBH gene target (Figure 6A). *Kiss1* gene expression was significantly increased in the liver of CREBH-Tg mice compared with WT mice (Figure 6B), which did not change even with deficiency of FGF21 (Figure 6B). Conversely, CREBH KO mice showed a significant reduction of *Kiss1* expression in the liver compared with WT mice in the fasting condition (Figure 6C). To determine whether CREBH directly regulates *Kiss1* expression, promoter analysis including luciferase assay, electrophoretic mobility shift assay (EMSA), and chromatin immunoprecipitation (ChIP) assay was performed. CREBH can bind to the cyclic AMP response element (CRE) sequence (Nakagawa et al., 2016b; Omori et al., 2001). A previous report revealed that mouse *Kiss1* promoter has two CRE sites (Song et al., 2014). In the luciferase analysis, CREBH activated *Kiss1* promoter activity but blunted it using the Kiss1 luciferase vectors deleting two putative CRE sites (Figure 6D). Consistent with these results, CREBH bound to both the putative CREBH-binding sites using EMSA (Figure 6E). Next, we performed the ChIP assay using AML12 cells infected with adenoviral CREBH. Surely, CREBH bound to *Kiss1* promoter (Figure 6F). Taken together, these results confirmed that *Kiss1* is a target for CREBH.

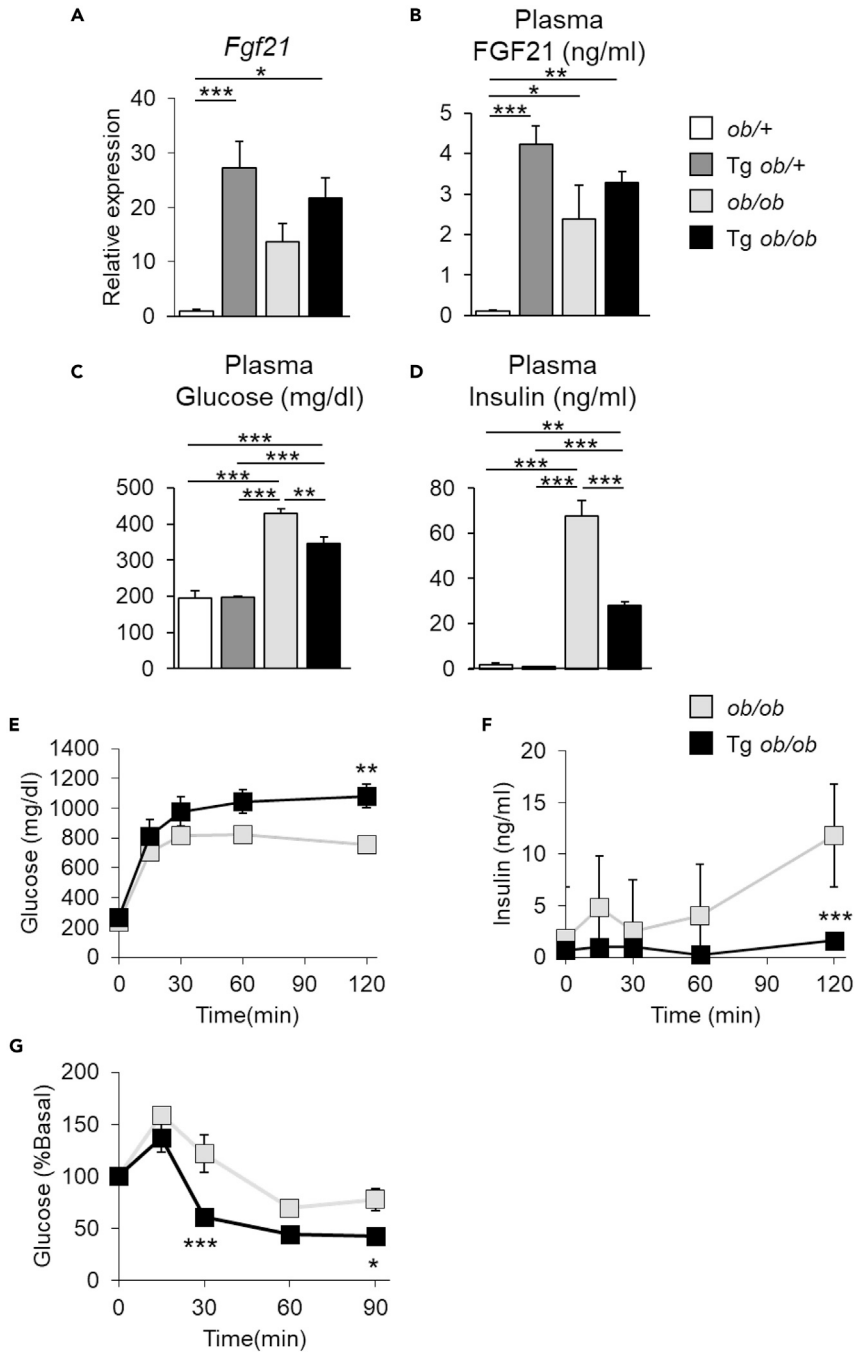

Figure 5. CREBH Ameliorates Glucose Metabolism in *ob/ob* Mice

(A) mRNA expressions of *Fgf21* of 10-week-old *ob/+*, Tg *ob/+*, *ob/ob*, and Tg *ob/ob* mice were determined by real-time PCR (n = 5–7).

(B–D) Plasma levels of FGF21 (n = 4–6) (B), glucose (n = 5–7) (C), and insulin (n = 3–6) (D).

(E and F) Plasma glucose levels (E) and insulin levels (F) during glucose tolerance test (GTT) in *ob/+*, Tg *ob/+*, *ob/ob*, and Tg *ob/ob* mice (n = 4–5).

(G) Blood glucose levels during insulin tolerance test (ITT) in *ob/+*, Tg *ob/+*, *ob/ob*, and Tg *ob/ob* mice (n = 7–8). Results are represented as means ± SEM. *p < 0.05, **p < 0.01, ***p < 0.001.

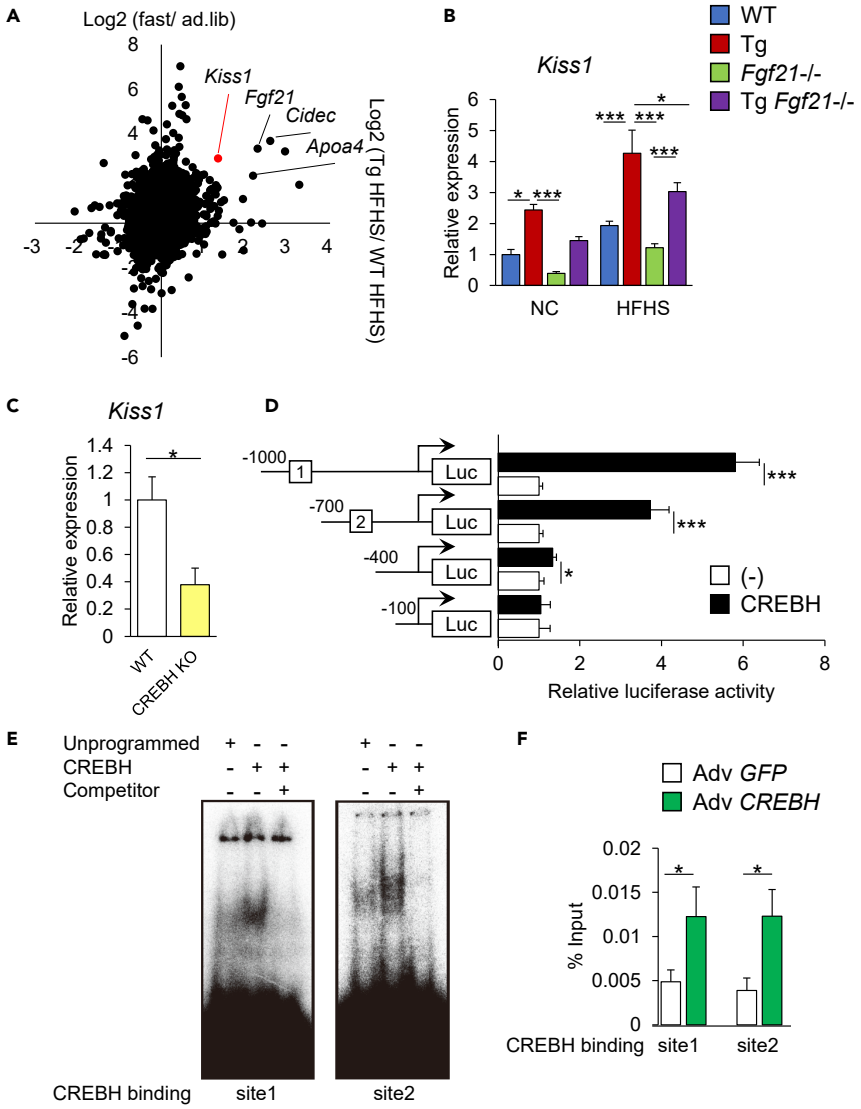

Figure 6. *Kiss1* Is a New Target for CREBH

(A) Microarray analysis from two independent datasets from liver samples. Relative gene expression of Tg mice fed HFHS diet for 12 weeks from age 6 weeks divided by WT mice fed HFHS diet for 12 weeks from age 6 weeks (log2, x axis), and WT mice fasted for 24 h divided by *ad lib* (log2, y axis).

(B) mRNA expressions of *Kiss1* gene in the liver from WT, Tg, *Fgf21*$^{-/-}$, and Tg *Fgf21*$^{-/-}$ mice fed normal chow or HFHS diet for 12 weeks from age 6 weeks were determined by real-time PCR (n = 7–8).

(C) mRNA expressions of *Kiss1* gene in 8-week-old 24-h-fasted liver from WT and *CrebH*$^{-/-}$ mice were determined by real-time PCR (n = 4–9).

(D) Mouse *Kiss1* promoter activity in AML 12.2 cells, as estimated by luciferase reporter assay. AML 12.2 cells were transfected with a pGL4.10-*Kiss1* reporter with 300-bp deletion series from 1000 bp and the indicated expression plasmid (n = 8).

(E) EMSA analysis of the CREBH-binding sites in the *Kiss1* gene promoter. The *in vitro*-translated CREBH protein and ^{32}P-labeled oligonucleotides for the CREBH-binding site 1 and site 2 were used in EMSAs.

(F) Chromatin immunoprecipitation (ChIP) assays were performed with anti-hemagglutinin (HA) antibodies from Adv *GFP*- or Adv HA *CrebH*-treated AML 12.2 cells (n = 5). Results are represented as means ± SEM. *p < 0.05, ***p < 0.001.

CREBH-Induced Kiss1 Contributes to Insulin Sensitivity

To determine the role of Kiss1 induced by CREBH, 7-week HFHS-diet-fed *Fgf21*$^{-/-}$ and CREBH-Tg *Fgf21*$^{-/-}$ mice were infected with Kiss1 knockdown adenovirus (Adv *Kiss1i*). At 4 weeks after adenovirus

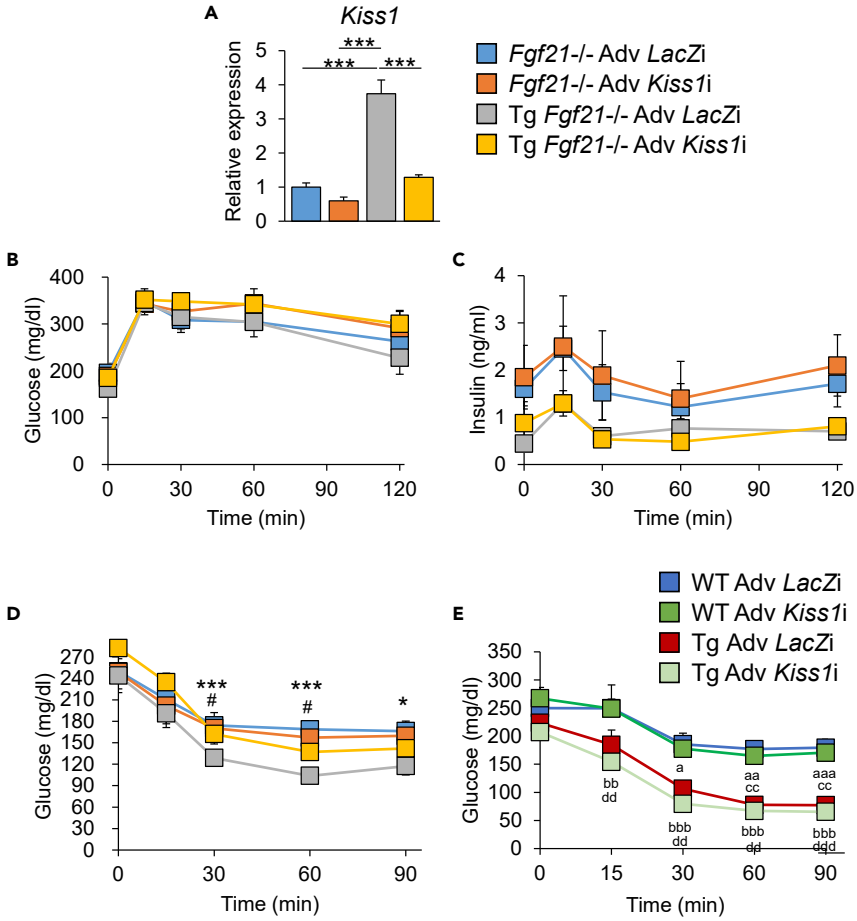

Figure 7. Adenoviral *Kiss1* Knockdown in the Liver of Tg *Fgf21*KO Mice Fed an HFHS Diet Attenuates Insulin Sensitivity

(A) *Fgf21*$^{-/-}$ and Tg *Fgf21*$^{-/-}$ mice fed an HFHS diet for 7 weeks from age 6 weeks and then infected with Adv *LacZi* or Adv *Kiss1*i. At 4 weeks after treatment, mRNA expressions of *Kiss1* gene in the liver from these mice were determined by real-time PCR (n = 5–7). ***p < 0.001.

(B and C) (B) Plasma glucose levels and (C) plasma insulin levels during glucose tolerance test (GTT) in *Fgf21*$^{-/-}$ and Tg *Fgf21*$^{-/-}$ mice 3 weeks after treatment with Adv *LacZi* or Adv *Kiss1*i (n = 5–7).

(D) Blood glucose levels during insulin tolerance test (ITT) in *Fgf21*$^{-/-}$ and Tg *Fgf21*$^{-/-}$ mice 3 weeks after treatment with Adv *LacZi* or Adv *Kiss1*i (n = 5–7). *Statistical significance between *Fgf21*$^{-/-}$ Adv *LacZi* and Tg *Fgf21*$^{-/-}$ Adv *LacZi* mice (*p < 0.05, ***p < 0.001). $^{\#}$Statistical significance between Tg *Fgf21*$^{-/-}$ Adv *LacZi* and Tg *Fgf21*$^{-/-}$ Adv *Kiss1*i mice ($^{\#}$p < 0.05). Results are represented as means ± SEM.

(E) Blood glucose levels during ITT in WT and Tg mice 3 weeks after treatment with Adv *LacZi* or Adv *Kiss1*i (n = 6–7). ^{a}Statistical significance between WT Adv *LacZi* and Tg Adv *LacZi* mice (^{a}p < 0.05, ^{aa}p < 0.01, ^{aaa}p < 0.001). ^{b}Statistical significance between WT Adv *LacZi* and Tg Adv *Kiss1*i mice (^{bb}p < 0.01, ^{bbb}p < 0.001). ^{c}Statistical significance between WT Adv *Kiss1i* and Tg Adv *LacZi* mice (^{cc}p < 0.01). ^{d}Statistical significance between WT Adv *Kiss1*i and Tg Adv *Kiss1*i mice (^{dd}p < 0.01, ^{ddd}p < 0.001). Results are represented as means ± SEM.

infection, we confirmed that *Kiss1* expression in the liver of CREBH-Tg *Fgf21*$^{-/-}$ mice was reduced to the same level as that in *Fgf21*$^{-/-}$ mice infected with Adv *LacZi* (Figure 7A). GTT was performed at 3 weeks after adenovirus infection. There were no differences in plasma glucose levels among all mouse genotype groups (Figure 7B). Plasma insulin levels during GTT were lower in CREBH-Tg *Fgf21*$^{-/-}$ mice compared with *Fgf21*$^{-/-}$ mice irrespective of adenovirus treatment (Figure 7C). At 3 weeks after adenovirus infection, ITT was performed. CREBH-Tg *Fgf21*$^{-/-}$ Adv *LacZi* mice had lower plasma glucose levels than *Fgf21*$^{-/-}$ Adv *LacZi* mice. Administration of Adv-Kiss1i treatment to CREBH-Tg *Fgf21*$^{-/-}$ (CREBH-Tg *Fgf21*$^{-/-}$ Adv *Kiss1i*) mice gave rise to consistently higher glucose levels than CREBH-Tg *Fgf21*$^{-/-}$ Adv *LacZi* mice, canceling the blood glucose-lowering effect of CREBH overexpression (Figure 7D). These findings

indicate that Kiss1 contributes to CREBH-induced insulin sensitivity. CREBH-Tg mice had lower plasma glucose levels than WT mice even if infected with Adv *Kiss1i* (Figure 7E). In the presence of FGF21, Adv *Kiss1i* did not suppress CREBH-induced insulin sensitivity. Taken together, FGF21 and Kiss1 might cooperate in CREBH-mediated improvement of glucose metabolism.

DISCUSSION

In this study, we analyzed the improvement of DIO phenotypes by CREBH overexpression described in our previous report (Nakagawa et al., 2014), using CREBH-Tg, *Fgf21*$^{-/-}$ and CREBH-Tg *Fgf21*$^{-/-}$ mice. Anti-obesity effect of CREBH was mediated by the activation of FGF21. Deficiency of FGF21 in CREBH-Tg mice canceled out CREBH-induced obesity phenotypes, confirming that FGF21 is crucial in CREBH-mediated amelioration of DIO. However, CREBH-Tg *Fgf21*$^{-/-}$ mice still sustained some improved phenotypes such as the suppression of inflammation in eWAT and amelioration of insulin resistance. These phenotypes are FGF21 independent. Notably, we identified that Kiss1 is a potential novel target of CREBH to improve insulin sensitivity. Collectively, we revealed that CREBH ameliorates DIO phenotypes in FGF21-dependent and FGF21-independent mechanisms.

There are the following pieces of previous literature to support the mechanism by which FGF21 mediates the phenotypes of CREBH-Tg mice. The phenotypes of high-fat diet-induced obesity were improved in FGF21-Tg mice (Owen et al., 2014). These phenotypes are reported to be canceled with the deficiency of βKlotho, a component of the FGF21 receptor complex, in both the hypothalamus and dorsal-vagal complex of FGF21-Tg mice (Owen et al., 2014). Secreted FGF21 can activate the sympathetic nervous system and activate lipolysis in WATs and thermogenesis by the conversion of WAT adipocytes to beige adipocytes. FGF21 directly activates PGC-1α and in turn increases *Ucp1* expression in adipocytes, leading to an increase in thermogenesis in these cells (Fisher et al., 2012). Consistent with these reports, CREBH-Tg mice revealed a marked increase of UCP1 mRNA and protein in the iWAT, subsequently increasing energy expenditure compared with WT mice. These changes were canceled in *Fgf21*$^{-/-}$ mice, thereby confirming that FGF21 mainly contributes to the thermogenic and anti-obesity phenotypes in CREBH-Tg mice.

It should be noticed that obesity mouse models, including *ob/ob*, *db/db*, and DIO mice, showed FGF21 resistance because of down-regulation of βKlotho (Hale et al., 2012). Even though CREBH-Tg mice have chronic higher plasma FGF21 levels, CREBH-Tg overexpression kept glucose and insulin levels lower in DIO, *ob/ob*, and *dbdb* mice (data not shown). In the current study, plasma glucose- and insulin-lowering effects of CREBH were observed even in DIO-induced CREBH-Tg *Fgf21*$^{-/-}$ and *ob/ob*; CREBH-Tg mice. Taken together, we hypothesized FGF21-independent pathway in improving insulin sensitivity by CREBH to identify Kiss1.

On feeding with high-fat diet, mice overexpressing Cidea in WATs develop obesity, but enhance insulin sensitivity, suggesting that these mice develop metabolic healthy obesity (Abreu-Vieira et al., 2015). Likewise, CREBH overexpression increased *Cidea* expression in eWAT and iWAT of both WT and *Fgf21*$^{-/-}$ mice. Although BWs of CREBH-Tg *Fgf21*$^{-/-}$ mice were similar to those of *Fgf21*$^{-/-}$ mice, CREBH-Tg *Fgf21*$^{-/-}$ mice kept better insulin response than *Fgf21*$^{-/-}$ mice. Thus, *Cidea* induction in adipose tissues might be a contributing factor to insulin sensitivity in CREBH-Tg mice.

CREBH overexpression was associated with the suppression of macrophage infiltration in eWAT of both WT and *Fgf21*$^{-/-}$ background mice. Deficiency of FGF21 induced genes related to macrophages and inflammatory cytokines, but CREBH overexpression reversed these genes to the levels of WT mice. FGF21 activates Nrf2/HO-1 and suppresses nuclear factor (NF)-κB in macrophages, thereby inducing anti-inflammatory effects by enhancing Nrf2-mediated anti-oxidant capacity and suppressing NF-κB signaling pathway (Yu et al., 2016). The effects of CREBH overexpression on macrophage infiltration are independent of FGF21. Inflammation of macrophages in eWAT is known to affect insulin sensitivity, one of the major contributors to obesity-mediated metabolic disturbances. Consistently, *Fgf21*$^{-/-}$ mice showed both high glucose and insulin levels during GTT, indicating that *Fgf21*$^{-/-}$ mice will likely progress to severe impairment of glucose response.

We identified *Kiss1* as a novel CREBH target gene responsible for better insulin sensitivity and glucose metabolism even in the absence of FGF21. Besides the major well-known role as a hypothalamus

neuropeptide sex hormone, there have been some conflicting reports on the functions of Kiss1 in insulin action: whereas it is reported to inhibit or activate insulin secretion from the islets (Hauge-Evans et al., 2006; Song et al., 2014), Kiss1 receptor KO mice exhibit adiposity, hyperleptinemia, and reduced energy expenditure (Tolson et al., 2016), thereby leading to glucose intolerance and obesity. These reports suggest that Kisspeptin signaling is important in peripheral tissues such as WAT and BAT, activating energy expenditure through thermogenesis. Exogenous Kiss1 administration to monkeys increases plasma adiponectin levels (Wahab et al., 2011). Adiponectin cooperates with FGF21 to improve glucose metabolism and insulin sensitivity in mice (Lin et al., 2013). These support a possibility that the effects of CREBH on adipose tissues partially contribute to Kiss1. Consistently. the knockdown of Kiss1 in CREBH-Tg *Fgf21*$^{-/-}$ mice partially canceled CREBH-mediated glucose-lowering effects in ITT, proposing that Kiss1 might be a CREBH-mediated insulin sensitizer. However, we need to further investigate the roles of Kiss1 on energy metabolism.

In this study, we revealed that CREBH increases hepatic expression and plasma levels of FGF21, leading to the activation of browning and subsequent thermogenesis in iWAT. CREBH suppresses inflammation of eWAT independent of FGF21. Moreover, CREBH induces its novel target *Kiss1* expression and then activates insulin sensitivity. Finally, we propose that hepatic CREBH improves DIO-mediated dysfunctions in peripheral tissues by improving systemic energy metabolism in FGF21-dependent and FGF21-independent mechanism. These findings indicate that CREBH has pleiotropic effects on obesity and diabetes. Further research to identify further unknown factors in FGF21-independent pathway should be the next project.

Limitations of the Study

CREBH has pleiotropic effects on obesity and diabetes in FGF21-dependent and FGF21-independent mechanisms. We evaluated CREBH-mediated mechanisms using CREBH-Tg *Fgf21*$^{-/-}$ mice. In this study, we identified that Kiss1 is a CREBH-mediated FGF21-independent insulin sensitizer. However, there are still unknown CREBH-mediated FGF21-independent mechanisms. Further research to identify further unknown factors in FGF21-independent pathway should be the next project.

METHODS

All methods can be found in the accompanying Transparent Methods supplemental file.

DATA AND CODE AVAILABILITY

The data discussed in this publication have been deposited in NCBI's Gene Expression Omnibus (GEO, http://www.ncbi.nlm.nih.gov/geo/) and are accessible through GEO Series accession number GSE143420 and GSE143421.

SUPPLEMENTAL INFORMATION

Supplemental Information can be found online at https://doi.org/10.1016/j.isci.2020.100930.

ACKNOWLEDGMENTS

This work was supported by Grants-in-Aid from the Ministry of Science, Education, Culture and Technology of Japan (to A.S.: Research Activity start-up 17H06541, to S.-i.H.: Research Activity start-up 26882008, to H.I.: Scientific Research (C) 16K09738 and 19K11737, to Y.N.: Scientific Research (B) 25282214 and 16H03253, to H.S.: Scientific Research (A) 15H02541 and 18H04051 and Scientific Research on Innovative Areas [Research in a proposed research area] Preventive medicine through inflammation cellular sociology 17H06395), AMED-CREST (to H.S.), Takeda Science Foundation (to Y.N.), Mochida Memorial Foundation for Medical and Pharmaceutical Research (to Y.N.), ONO Medical Research Foundation (to Y.N.), Japan Foundation for Applied Enzymology (to Y.N.), and Suzuken Memorial Foundation (to Y.N.). This manuscript was edited and proofread by Enago.

AUTHOR CONTRIBUTIONS

S.-i.H., Y.N., and H. Shimano designed the experiments and wrote the manuscript. A.S., S.-i.H., M.A., Y.N., H.O., and K.K. performed the experiments. A.S., S.-i.H., and Y.N. analyzed and interpreted the data. M.K.,

and N.I. generated *Fgf21*$^{-/-}$ mice. Y. Mizunoe, Y. Murayama, Y.O., H.I., M.S., T.M., and H. Sone were involved in the project planning and the discussion.

DECLARATION OF INTERESTS

The authors declare no competing interests.

Received: October 3, 2019
Revised: January 16, 2020
Accepted: February 17, 2020
Published: March 27, 2020

REFERENCES

Abreu-Vieira, G., Fischer, A.W., Mattsson, C., de Jong, J.M., Shabalina, I.G., Ryden, M., Laurencikiene, J., Arner, P., Cannon, B., Nedergaard, J., et al. (2015). Cidea improves the metabolic profile through expansion of adipose tissue. Nat. Commun. *6*, 7433.

Badman, M.K., Pissios, P., Kennedy, A.R., Koukos, G., Flier, J.S., and Maratos-Flier, E. (2007). Hepatic fibroblast growth factor 21 is regulated by PPARalpha and is a key mediator of hepatic lipid metabolism in ketotic states. Cell Metab. *5*, 426–437.

Chau, M.D., Gao, J., Yang, Q., Wu, Z., and Gromada, J. (2010). Fibroblast growth factor 21 regulates energy metabolism by activating the AMPK-SIRT1-PGC-1alpha pathway. Proc. Natl. Acad. Sci. U S A *107*, 12553–12558.

Danno, H., Ishii, K.A., Nakagawa, Y., Mikami, M., Yamamoto, T., Yabe, S., Furusawa, M., Kumadaki, S., Watanabe, K., Shimizu, H., et al. (2010). The liver-enriched transcription factor CREBH is nutritionally regulated and activated by fatty acids and PPARalpha. Biochem. Biophys. Res. Commun. *391*, 1222–1227.

Fisher, F.M., Chui, P.C., Antonellis, P.J., Bina, H.A., Kharitonenkov, A., Flier, J.S., and Maratos-Flier, E. (2010). Obesity is a fibroblast growth factor 21 (FGF21)-resistant state. Diabetes *59*, 2781–2789.

Fisher, F.M., Kleiner, S., Douris, N., Fox, E.C., Mepani, R.J., Verdeguer, F., Wu, J., Kharitonenkov, A., Flier, J.S., Maratos-Flier, E., et al. (2012). FGF21 regulates PGC-1alpha and browning of white adipose tissues in adaptive thermogenesis. Genes Dev. *26*, 271–281.

Gottsch, M.L., Cunningham, M.J., Smith, J.T., Popa, S.M., Acohido, B.V., Crowley, W.F., Seminara, S., Clifton, D.K., and Steiner, R.A. (2004). A role for kisspeptins in the regulation of gonadotropin secretion in the mouse. Endocrinology *145*, 4073–4077.

Hale, C., Chen, M.M., Stanislaus, S., Chinookoswong, N., Hager, T., Wang, M., Veniant, M.M., and Xu, J. (2012). Lack of overt FGF21 resistance in two mouse models of obesity and insulin resistance. Endocrinology *153*, 69–80.

Hauge-Evans, A.C., Richardson, C.C., Milne, H.M., Christie, M.R., Persaud, S.J., and Jones, P.M. (2006). A role for kisspeptin in islet function. Diabetologia *49*, 2131–2135.

Hondares, E., Iglesias, R., Giralt, A., Gonzalez, F.J., Giralt, M., Mampel, T., and Villarroya, F. (2011). Thermogenic activation induces FGF21 expression and release in brown adipose tissue. J. Biol. Chem. *286*, 12983–12990.

Hotta, Y., Nakamura, H., Konishi, M., Murata, Y., Takagi, H., Matsumura, S., Inoue, K., Fushiki, T., and Itoh, N. (2009). Fibroblast growth factor 21 regulates lipolysis in white adipose tissue but is not required for ketogenesis and triglyceride clearance in liver. Endocrinology *150*, 4625–4633.

Inagaki, T., Dutchak, P., Zhao, G., Ding, X., Gautron, L., Parameswara, V., Li, Y., Goetz, R., Mohammadi, M., Esser, V., et al. (2007). Endocrine regulation of the fasting response by PPARalpha-mediated induction of fibroblast growth factor 21. Cell Metab. *5*, 415–425.

Kharitonenkov, A., Wroblewski, V.J., Koester, A., Chen, Y.F., Clutinger, C.K., Tigno, X.T., Hansen, B.C., Shanafelt, A.B., and Etgen, G.J. (2007). The metabolic state of diabetic monkeys is regulated by fibroblast growth factor-21. Endocrinology *148*, 774–781.

Kim, H., Mendez, R., Zheng, Z., Chang, L., Cai, J., Zhang, R., and Zhang, K. (2014). Liver-enriched transcription factor CREBH interacts with peroxisome proliferator-activated receptor alpha to regulate metabolic hormone FGF21. Endocrinology *155*, 769–782.

Lee, J.H., Giannikopoulos, P., Duncan, S.A., Wang, J., Johansen, C.T., Brown, J.D., Plutzky, J., Hegele, R.A., Glimcher, L.H., and Lee, A.H. (2011). The transcription factor cyclic AMP-responsive element-binding protein H regulates triglyceride metabolism. Nat. Med. *17*, 812–815.

Li, H., Wu, G., Fang, Q., Zhang, M., Hui, X., Sheng, B., Wu, L., Bao, Y., Li, P., Xu, A., et al. (2018). Fibroblast growth factor 21 increases insulin sensitivity through specific expansion of subcutaneous fat. Nat. Commun. *9*, 272.

Lin, Z., Tian, H., Lam, K.S., Lin, S., Hoo, R.C., Konishi, M., Itoh, N., Wang, Y., Bornstein, S.R., Xu, A., et al. (2013). Adiponectin mediates the metabolic effects of FGF21 on glucose homeostasis and insulin sensitivity in mice. Cell Metab. *17*, 779–789.

Nakagawa, Y., Oikawa, F., Mizuno, S., Ohno, H., Yagishita, Y., Satoh, A., Osaki, Y., Takei, K., Kikuchi, T., Han, S.I., et al. (2016a). Hyperlipidemia and hepatitis in liver-specific CREB3L3 knockout mice generated using a one-step CRISPR/Cas9 system. Sci. Rep. *6*, 27857.

Nakagawa, Y., Satoh, A., Tezuka, H., Han, S.I., Takei, K., Iwasaki, H., Yatoh, S., Yahagi, N., Suzuki, H., Iwasaki, Y., et al. (2016b). CREB3L3 controls fatty acid oxidation and ketogenesis in synergy with PPARalpha. Sci. Rep. *6*, 39182.

Nakagawa, Y., Satoh, A., Yabe, S., Furusawa, M., Tokushige, N., Tezuka, H., Mikami, M., Iwata, W., Shingyouchi, A., Matsuzaka, T., et al. (2014). Hepatic CREB3L3 controls whole-body energy homeostasis and improves obesity and diabetes. Endocrinology *155*, 4706–4719.

Omori, Y., Imai, J., Watanabe, M., Komatsu, T., Suzuki, Y., Kataoka, K., Watanabe, S., Tanigami, A., and Sugano, S. (2001). CREB-H: a novel mammalian transcription factor belonging to the CREB/ATF family and functioning via the box-B element with a liver-specific expression. Nucleic Acids Res. *29*, 2154–2162.

Owen, B.M., Ding, X., Morgan, D.A., Coate, K.C., Bookout, A.L., Rahmouni, K., Kliewer, S.A., and Mangelsdorf, D.J. (2014). FGF21 acts centrally to induce sympathetic nerve activity, energy expenditure, and weight loss. Cell Metab. *20*, 670–677.

Park, J.G., Xu, X., Cho, S., Hur, K.Y., Lee, M.S., Kersten, S., and Lee, A.H. (2016). CREBH-FGF21 axis improves hepatic steatosis by suppressing adipose tissue lipolysis. Sci. Rep. *6*, 27938.

Song, W.J., Mondal, P., Wolfe, A., Alonso, L.C., Stamateris, R., Ong, B.W., Lim, O.C., Yang, K.S., Radovick, S., Novaira, H.J., et al. (2014). Glucagon regulates hepatic kisspeptin to impair insulin secretion. Cell Metab. *19*, 667–681.

Tolson, K.P., Garcia, C., Delgado, I., Marooki, N., and Kauffman, A.S. (2016). Metabolism and energy expenditure, but not feeding or glucose tolerance, are impaired in young Kiss1r KO female mice. Endocrinology *157*, 4192–4199.

Veniant, M.M., Sivits, G., Helmering, J., Komorowski, R., Lee, J., Fan, W., Moyer, C., and Lloyd, D.J. (2015). Pharmacologic effects of FGF21 are independent of the "browning" of white adipose tissue. Cell Metab. *21*, 731–738.

Wahab, F., Riaz, T., and Shahab, M. (2011). Study on the effect of peripheral kisspeptin administration on basal and glucose-induced insulin secretion under fed and fasting conditions in the adult male rhesus monkey (Macaca mulatta). Horm. Metab. Res. *43*, 37–42.

Wang, N., Xu, T.Y., Zhang, X., Li, J.Y., Wang, Y.X., Guo, X.C., Li, S.M., Wang, W.F., and Li, D.S. (2018). Improving hyperglycemic effect of FGF-21 is associated with alleviating inflammatory state in diabetes. Int. Immunopharmacol. *56*, 301–309.

Xu, J., Lloyd, D.J., Hale, C., Stanislaus, S., Chen, M., Sivits, G., Vonderfecht, S., Hecht, R., Li, Y.S., Lindberg, R.A., et al. (2009). Fibroblast growth factor 21 reverses hepatic steatosis, increases energy expenditure, and improves insulin sensitivity in diet-induced obese mice. Diabetes *58*, 250–259.

Yu, Y., He, J., Li, S., Song, L., Guo, X., Yao, W., Zou, D., Gao, X., Liu, Y., Bai, F., et al. (2016). Fibroblast growth factor 21 (FGF21) inhibits macrophage-mediated inflammation by activating Nrf2 and suppressing the NF-kappaB signaling pathway. Int. Immunopharmacol. *38*, 144–152.

Zhang, K., Shen, X., Wu, J., Sakaki, K., Saunders, T., Rutkowski, D.T., Back, S.H., and Kaufman, R.J. (2006). Endoplasmic reticulum stress activates cleavage of CREBH to induce a systemic inflammatory response. Cell *124*, 587–599.

Zhang, C., Wang, G., Zheng, Z., Maddipati, K.R., Zhang, X., Dyson, G., Williams, P., Duncan, S.A., Kaufman, R.J., and Zhang, K. (2012). Endoplasmic reticulum-tethered transcription factor cAMP responsive element-binding protein, hepatocyte specific, regulates hepatic lipogenesis, fatty acid oxidation, and lipolysis upon metabolic stress in mice. Hepatology *55*, 1070–1082.

iScience, Volume *23*

Supplemental Information

CREBH Improves Diet-Induced Obesity, Insulin Resistance, and Metabolic Disturbances by FGF21-Dependent and FGF21-Independent Mechanisms

Aoi Satoh, Song-iee Han, Masaya Araki, Yoshimi Nakagawa, Hiroshi Ohno, Yuhei Mizunoe, Kae Kumagai, Yuki Murayama, Yoshinori Osaki, Hitoshi Iwasaki, Motohiro Sekiya, Morichika Konishi, Nobuyuki Itoh, Takashi Matsuzaka, Hirohito Sone, and Hitoshi Shimano

Supplemental Information

CREBH improves diet-induced obesity, insulin resistance, and metabolic disturbances by FGF21-dependent and -independent mechanisms

Aoi Satoh, Song-iee Han, Masaya Araki, Yoshimi Nakagawa, Hiroshi Ohno, Yuhei Mizunoe, Kae Kumagai, Yuki Murayama, Yoshinori Osaki, Hitoshi Iwasaki, Motohiro Sekiya, Morichika Konishi, Nobuyuki Itoh, Takashi Matsuzaka, Hirohito Sone, Hitoshi Shimano

Transparent Methods

Animals

To generate the active form of human CREBH transgenic (CREBH-Tg) mice, cDNA encoding the rat *Pck1* promoter (Shimano et al., 1996), human CREBH (1–320 aa), and the 3′ polyadenylation signal of human growth hormone were microinjected into C57BL6J eggs (Nakagawa et al., 2014). *Fgf21*$^{-/-}$ mice were generated as previously described (Hotta et al., 2009). To generate CREBH-Tg *Fgf21*$^{-/-}$ mice, *Fgf21*$^{-/-}$ mice were crossed with CREBH-Tg mice. *CrebH*$^{-/-}$ mice (Luebke-Wheeler et al., 2008) were purchased from Jackson Lab.

For HFHS diet feeding analysis, 6-week-old male mice were fed for 12 weeks and sacrificed in a fed state. HFHS diet consisted 54.5% fat, 17.2% protein, and 28.3% carbohydrates (kcal%). ob/ob mice were purchased from CHARLES RIVER LABORATORIES JAPAN, INC. (Yokohama, JAPAN). To generate CREBH-Tg; *ob/ob* mice, *ob/ob* mice were crossed with CREBH-Tg mice. Oxygen consumption was measured by indirect calorimetry using the ARCO-2000 Mass Spectrometer (ARCO System). Rectal core temperature was measured with the rectal probe (RET-3; Physitemp) by a digital thermometer.

For adenoviral infection, 13-week-old male mice fed HFHS diet for 7 weeks from 6-week-old age were infected with the indicated adenovirus at 7.0×10^{11} opu/mouse, following which samples were collected at 4 weeks after infection from mice in a fed state.

All animal husbandry procedures and animal experiments were performed in accordance with the Regulation of Animal Experiments of the University of Tsukuba and were approved by the Animal Experiment Committee, University of Tsukuba.

Plasmids

The active form of human *CREBH* (1–320 aa) was cloned using PCR into the pcDNA3 vector. 1kb of the 5′ untranslated region of the mouse *Kiss1* gene were cloned using PCR and subcloned into the pGL4.10 [*luc2*] vector (Promega).

Preparation of recombinant adenovirus

Kiss1 RNAi was subcloned into pENTR TOPO U6 vector (ThermoScientific). *Kiss1* RNAi 350 sequence is 5′-CACCTACAACTGGAACTCC-3′. The recombinant adenoviruses were produced in 293A cells (Invitrogen) and purified using CsCl gradient centrifugation, as previously described (Nakagawa et al., 2006).

Metabolic measurements

For glucose tolerance test (GTT), mice were fasted for 16h (overnight) and then injected intraperitoneally with D-glucose 1 g per kg body weight. The insulin resistance index HOMA-R was

calculated on the basis of the fasting glucose and insulin levels. For insulin tolerance test (ITT), 4 h-fasted mice were injected intraperitoneally with human regular insulin (Eli Lilly) 0.5 U/kg body weight. Plasma glucose and insulin levels were measured as previously described (Nakagawa et al., 2006).

Immunoblotting

Total cell lysates were immunoblotted as previously described (Nakagawa et al., 2006), using antibodies to UCP1 (Abcam ab10983), and α-tubulin (Millipore 05-829).

Histological Analysis

Liver and adipose tissues were removed, fixed in 10% buffered formalin, embedded in paraffin, cut into 4- or 6-μm thick sections for the liver and adipose tissue, respectively, and stained with hematoxylin and eosin (H&E). Immunohistochemical staining for F4/80 (Abcam, ab6640) and UCP1 (Abcam ab10983) was performed as previously described (Ohno et al., 2018). All images were acquired using a BZ-8100 microscope (Keyence, Osaka, Japan).

Analysis of gene expression

Total RNA from tissues was prepared using Sepasol (Nacalai). The real-time PCR analysis was performed using total RNA for cDNA synthesis (Takara) with the ABI Prism 7300 system (ABI) and KAPA SYBR FAST qPCR Kit (Kapa Biosystems). Primer sequences are listed in Table S1.

Microarray analysis.

Total RNA from tissues was prepared using Sepasol. To determine the quality of RNA, the RNA Integrity Number (RIN) was measured using the Agilent 2100 Bioanalyzer. Microarray analysis was performed with the SurePrint G3 Mouse Gene Expression 8X60K Microarray Kit (Agilent Technologies).

Promoter analysis

Mouse AML12.2 hepatoma cells were transfected with the indicated luciferase reporter, expression plasmids, and a pRL-SV40 plasmid (Promega) as a reference using X-tremeGENE 9 (Roche). After a 24-h incubation, the firefly luciferase activity was measured and normalized to the *Renilla* luciferase activity. We generated CREBH from an expression vector using an *in vitro* reticulocyte transcription–translation system (Promega). We used the following sequences in the EMSAs: 5′-TGCTACCCTAGGTGCAGTAGACCCCTCCC-3′ and 5′-ACAAGAGAACACTGAGACACCCAGG-3′. We incubated the *in vitro*-translated protein lysate in a reaction mixture as previously described (Nakagawa et al., 2006) and resolved the DNA-protein complexes on a 4% polyacrylamide gel.

ChIP assay

ChIP assays were performed as previously described (Nakagawa et al., 2006). In brief, AML12.2 cells were infected with adenovirus GFP or the active form of CREBH tagged with HA in the N-terminus at a multiplicity of infection of 100, then incubated for 48 h. The soluble chromatin was subjected to immunoprecipitation with anti-HA (Y-11, Santa Cruz) and rotated overnight at 4 °C. Immune complexes were washed and then incubated overnight at 65 °C for reverse crosslinking. Chromatin DNA was extracted with phenol-chloroform, precipitated with ethanol, resuspended in water, and subjected to real-time PCR analysis. The primers used for real-time PCR were as follows: *Kiss1* promoter region containing the CREBH binding site 1, 5′-TGTCGTCTTTGGCTTCCT-3′ and 5′-TGCACCTAGGGTAGCAC-3′; site2, 5′-GTCTGGGCTACAGGCATAG-3′ and 5′-GCGATCCAAGCCGTGTGC-3′.

Statistical analyses

Statistical significance was calculated using unpaired Student's *t*-tests for single comparisons (Figure 5E-G, 6C, 6D, 6F, 7D left) and ANOVA followed by the Bonferroni test for multiple comparisons with a significance level of $P < 0.05$. All data are expressed as mean ± standard error of the mean (SEM).

Supplemental References

Hotta, Y., Nakamura, H., Konishi, M., Murata, Y., Takagi, H., Matsumura, S., Inoue, K., Fushiki, T., and Itoh, N. (2009). Fibroblast growth factor 21 regulates lipolysis in white adipose tissue but is not required for ketogenesis and triglyceride clearance in liver. Endocrinology *150*, 4625-4633.

Luebke-Wheeler, J., Zhang, K., Battle, M., Si-Tayeb, K., Garrison, W., Chhinder, S., Li, J., Kaufman, R.J., and Duncan, S.A. (2008). Hepatocyte nuclear factor 4alpha is implicated in endoplasmic reticulum stress-induced acute phase response by regulating expression of cyclic adenosine monophosphate responsive element binding protein H. Hepatology *48*, 1242-1250.

Nakagawa, Y., Satoh, A., Yabe, S., Furusawa, M., Tokushige, N., Tezuka, H., Mikami, M., Iwata, W., Shingyouchi, A., Matsuzaka, T., et al. (2014). Hepatic CREB3L3 Controls Whole-Body Energy Homeostasis and Improves Obesity and Diabetes. Endocrinology *155*, 4706-4719.

Nakagawa, Y., Shimano, H., Yoshikawa, T., Ide, T., Tamura, M., Furusawa, M., Yamamoto, T., Inoue, N., Matsuzaka, T., Takahashi, A., et al. (2006). TFE3 transcriptionally activates hepatic IRS-2, participates in insulin signaling and ameliorates diabetes. Nat Med *12*, 107-113.

Ohno, H., Matsuzaka, T., Tang, N., Sharma, R., Motomura, K., Shimura, T., Satoh, A., Han, S.I., Takeuchi, Y., Aita, Y., et al. (2018). Transgenic Mice Overexpressing SREBP-1a in Male ob/ob Mice Exhibit Lipodystrophy and Exacerbate Insulin Resistance. Endocrinology *159*, 2308-2323.

Shimano, H., Horton, J.D., Hammer, R.E., Shimomura, I., Brown, M.S., and Goldstein, J.L. (1996). Overproduction of cholesterol and fatty acids causes massive liver enlargement in transgenic mice expressing truncated SREBP-1a. J Clin Invest *98*, 1575-1584.

Table S1 Primers used for real-time PCR analysis. Related to Figure 1–3, 5, and 6.

Acox1	Fw CGA TCC AGA CTT CCA ACA TGA G
	Rv CCA TGG TGG CAC TCT TCT TAA CA
ApoA4	Fw TTA CCC AGC TAA GCA ACA ATG C
	Rv GAG GGT ACT GAG CTG CTG AGT GA
ApoC2	Fw CCA AGG AGC TTG CCA AAG AC
	Rv TGC CTG CGT AAG TGC TCA TG
ApoC3	Fw TAG AGG GCT ACA TGG AAC AAG C
	Rv CAG GGA TCT GAA GTG ATT GTC C
Ccl2	Fw CCC ACT CAC CTG CTG CTA CT
	Rv ATT TGG TTC CGA TCC AGG TT
Cd68	Fw CCT CCA CCC TCG CCT AGT C
	Rv TTG GGT ATA GGA TTC GGA TTT GA
Cidea	Fw CATCCCCCAAGCCTAG
	Rv CTCTGTAGCTGTGCCC
Cpt1a	Fw TCT TTC ACT GAG TTC CGA TGG G
	Rv ACG CCA GAG ATG CCT TTT CC
Cyclophillin	Fw TGG CTC ACA GTT CTT CAT AAC CA
	Rv ATG ACA TCC TTC AGT GGC TTG TC
Elovl3	Fw TTCTCACGCGGGTTAAAAATGG
	Rv GAGCAACAGATAGACGACCAC
Elovl6	Fw ACA ATG GAC CTG TCA GCA AA
	Rv GTA CCA GTG CAG GAA GAT CAG T
Fasn	Fw ATC CTG GAA CGA CGA GAA CAC GAT CT
	Rv AGA GAC GTG TCA TCC TGG ACT T
Fgf21	Fw AGA TCA GGG AGG ATG GAA CA
	Rv TCA AAG TGA GGC GAT CCA TA
Hmgcr	Fw GAG AAG AAG CCT GCT GCA TA
	Rv CGT CAA CCA TAG CTT CCG TAG TT
Hmgcs1	Fw GTG GCA CCG GAT GTC TTT G
	Rv CTC TGA CCA GAT ACC ACG TTC
Il6	Fw TAG TCC TTC CTA CCC CAA TTT CC
	Rv TTG GTC CTT AGC CAC TCC TTC
Lipe	Fw GAGCGCTGGAGGAGTGTTTT
	Rv TGATGCAGAGATTCCCACCTG

Pnpla2 Fw CAAAGGGTTGGGTTGGTTCAG

Pnpla2 Rv GGATGGCGGCATTTCAGACA

Ppara Fw CCT CAG GGT ACC ACT ACG GAG T

Ppara Rv GCC GAA TAG TTC GCC GAA

Pparg Fw TCAACATGGAATGTCGGGTG

Pparg Rv ATACTCGAGCTTCATGCGGATT

Ppargc1a Fw TTCAAGATCCTGTTACTACT

Ppargc1a Rv ACCTTGAACGTGATCTCACA

Prdm16 Fw GGCGAGGAAGCTAGCC

Prdm16 Rv GGTCTCCTCCTCGGCA

Scd1 Fw AGA TCT CCA GTT CTT ACA CGA CCA C

Scd1 Rv CTT TCA TTT CAG GAC GGA TGT CT

Srebf1 Fw CGGCGCGGAAGCTGT

Srebf1 Rv TGCA ATCCATGGCTCCGT

Srebf2 Fw CTG CAG CCT CAA GTG CAA AG

Srebf2 Rv CAG TGT GCC ATT GGC TGT CT

Tnf Fw TCG TAG CAA ACC ACC AAG TG

Tnf Rv AGA TAG CAA ATC GGC TGA CG